

LETTER • OPEN ACCESS

Single layer graphene induces load-bearing molecular layering at the hexadecane-steel interface

To cite this article: G Krämer *et al* 2019 *Nanotechnology* **30** 46LT01

View the [article online](#) for updates and enhancements.



IOP | ebooks™

Bringing you innovative digital publishing with leading voices to create your essential collection of books in STEM research.

Start exploring the collection - download the first chapter of every title for free.

Letter

Single layer graphene induces load-bearing molecular layering at the hexadecane-steel interface

G Krämer^{1,2}, C Kim^{3,4}, K-S Kim^{3,4}  and R Bennewitz ^{1,2}¹INM—Leibniz Institute for New Materials, Campus D2 2, D-66123 Saarbrücken, Germany²Physics Department, Saarland University, D-66123 Saarbrücken, Germany³Nano-Convergence Mechanical Systems Research Division, Korea Institute of Machinery & Materials (KIMM), 156 Gajeongbuk-ro, Yuseong-gu, Daejeon 34103, Republic of Korea⁴Department of Nanomechatronics, Korea University of Science & Technology (UST), 217 Gajeong-ro, Yuseong-gu, Daejeon 34113, Republic of KoreaE-mail: roland.bennewitz@leibniz-inm.de

Received 21 May 2019, revised 23 July 2019

Accepted for publication 19 August 2019

Published 2 September 2019



CrossMark

Abstract

The influence of a single layer graphene on the interface between a polished steel surface and the model lubricant hexadecane is explored by high-resolution force microscopy. Nanometer-scale friction is reduced by a factor of three on graphene compared to the steel substrate, with an ordered layer of hexadecane adsorbed on the graphene. Graphene furthermore induces a molecular ordering in the confined lubricant with an average range of 4–5 layers and with a strongly increased load-bearing capacity compared to the lubricant on the bare steel substrate.

Keywords: atomic force microscopy, graphene, molecular layering, nanotribology

(Some figures may appear in colour only in the online journal)

1. Introduction

Carbon-based layers play an important role in boundary lubrication, from graphite as commercial solid lubricant in a spray can over diamond-like carbon coatings in automotive industries [1] all the way to graphitic layers found in metal-metal hip implants [2]. With increasing availability of graphene, the two-dimensional building block of graphite, its possible role in lubrication is being explored. Single layers of graphene were studied by friction force microscopy and were found to reduce friction of a variety of substrates and environments at the nanometer scale, including epitaxial graphene on SiC in vacuum [3], exfoliated graphene on silica in dry

atmosphere [4], graphene grown by chemical-vapor deposition (CVD) on copper in air [5], or exfoliated graphene on silica in dodecane and water [6]. Lubrication by CVD-grown graphene has been demonstrated also on larger scale on silica [7]. After the discovery of friction and wear reduction on steel surfaces by graphene in a variety of environments [8], graphene is now emerging as new lubricant [9]. Polymer composites with graphene exhibit improved tribological properties due to wear reduction by efficient transfer layers [10]. The composite approach has been successfully extended to multilayers of polymer and graphene [11]. The use of graphene as additive in formulated lubricant oils is also promising after functionalization to improve solubility [12, 13].

In this letter, we report experimental results for fundamental lubrication properties of the interface between a hexadecane model lubricant and a steel surface modified by a single layer graphene. Using high-resolution force microscopy, we quantify that the reduction of friction on graphene



Original content from this work may be used under the terms of the [Creative Commons Attribution 3.0 licence](https://creativecommons.org/licenses/by/3.0/). Any further distribution of this work must maintain attribution to the author(s) and the title of the work, journal citation and DOI.

is connected to an ordered layer of adsorbed hexadecane molecules and that the graphene induces an ordering in molecular layers in the confined liquid above graphene patches.

2. Experimental

Stainless steel samples (X5CrNi18-10) were polished using diamond paste and colloidal silica suspension to a roughness of 0.78 nm rms as determined by AFM. Graphene was transferred to the steel surface via a dry-transfer process using a carrier film [14]. The graphene was grown on 35 μm thick Cu foil through a CVD process. The graphene/Cu foil was laminated on the carrier film that consisted of thin polydimethylsiloxane (PDMS) layer on polyethylene terephthalate (PET) film. Then, Cu was etched with ammonium persulfate (APS) and the graphene on PDMS/PET was transferred to the steel surface. The successful transfer of graphene was proven by high-resolution friction force microscopy images exhibiting the periodicity of the honeycomb lattice (data not shown).

All AFM measurements were performed at room temperature using an Agilent AFM 5500 with a home-built fluid cell where the cantilever is fully immersed in hexadecane (Sigma-Aldrich). Molecular sieves with a pore diameter of 0.3 nm were added to the hexadecane in order to minimize the water content. Rectangular silicon cantilevers (PPP-CONTR, Nanosensors, Neuchâtel, Switzerland) with a backside reflective aluminum coating, a nominal spring constant of 0.2 N m^{-1} , and a nominal tip radius $< 10 \text{ nm}$ were used. The individual spring constants were determined using Sader's method [15]. To record force-distance curves, the cantilever was approached slowly ($v < 2 \text{ nm s}^{-1}$) to the substrate surface until reaching a predefined maximum force and then retracted. The cantilever deflection was calibrated by determination of the slope of the force curve when the tip was in contact with the substrate. Lateral force were measured as the twist of the cantilever when scanning the tip in contact over the surface [16].

3. Results

Topography and friction contrast of the transition between a graphene flake and the steel substrate is shown in figure 1. The topography is dominated by the roughness of the steel substrate, to which the graphene layer adapts, and by folds in the graphene layer. While there is no particular contrast in the topographic features between graphene and steel substrate, the lateral force is significantly lower on graphene. We observe that in this boundary-lubrication regime, friction on steel in the model lubricant hexadecane is reduced by a factor of three on a single layer graphene. We will show in the following that the low-friction interface is an ordered layer of hexadecane on graphene.

Exemplary tip-approach curves for steel and graphene are compared in figure 2(a). The normal force is plotted as function of the tip-sample distance. The layering of

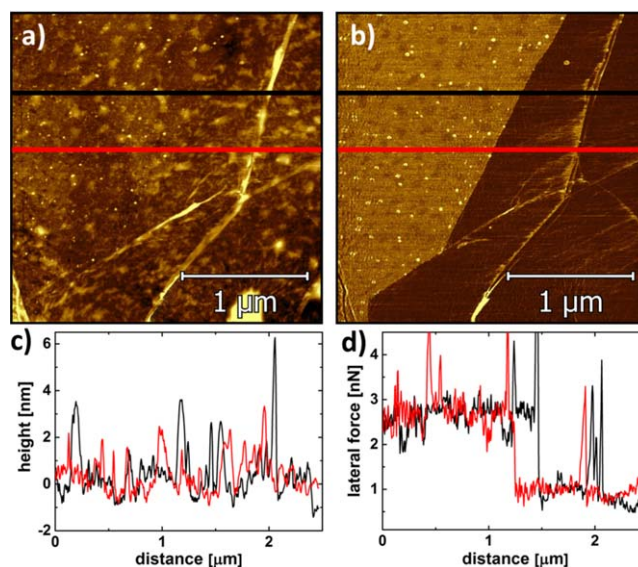


Figure 1. Force microscopy of a steel surface partially covered by graphene (lower right half of the frame). The image was recorded in hexadecane at a normal force of 1.5 nN. (a) Topography showing the roughness of the steel surface and folds in the graphene layer. (b) Friction contrast between steel (bright) and graphene (dark). (c) Topography cross-sections as indicated in (a) by lines in the respective color. (d) Friction force cross-sections as indicated in (b) by lines of the respective color. The cross-sections reveal a decrease in friction on graphene by a factor of three.

hexadecane is revealed by a series of steps. A certain normal force is required to penetrate each molecular layer. In the example for graphene, the tip advances from the fourth to the third layer at a force of 0.15 nN, from the third to the second at 0.35 nN, from the second to the last remaining layer at 1.75 nN. The tip does not penetrate the last layer at the forces applied in these approach curves, as we will discuss below. We have limited the maximum normal force to protect the tip integrity. Experiments on graphite have also reported forces larger than 5 nN for the penetration of the last layer of hexadecane, which was confirmed by simultaneous measurements of the electrical resistance between tip and sample [17].

The force steps are result of a tip-sample interaction potential which oscillates as function of the distance. This potential arises from molecular density fluctuations in the confinement. The resulting solvation forces acting on confining asperities have been predicted for linear alkanes by molecular dynamics simulations [18]. The distance jumps can be predicted by comparing the slopes of an exponentially decaying oscillatory solvation force with the cantilever stiffness [19]. The equilibrium character of the layering is revealed by the observation of jumps back and forth between the third and the fourth layer in figure 2(a) at a force around 0.25 nN. The average distance between the force jumps of 0.45 nm agrees with the expected width of the hexadecane molecule and reveals that the molecules arrange parallel to the confining surfaces. The histogram of tip-sample distances in the background of figure 2(a) visualizes the position of the layer. A small peak at a distance of 2.2 nm indicates even a fifth layer of hexadecane.

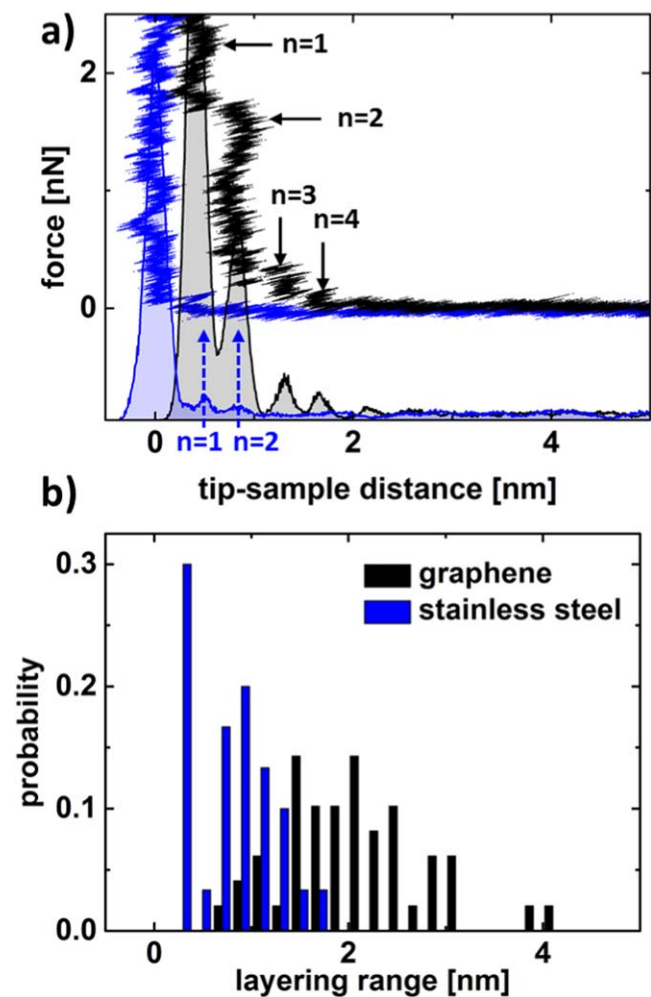


Figure 2. Summary of molecular layering of hexadecane on graphene and stainless steel. (a) Exemplary force-distance curves on graphene (black) and steel (blue). The shaded histograms in the background indicate the probability to find the tip at a certain distance from the sample during approach. The parameter n counts the number of hexadecane layer between tip and sample. (b) Histograms of the layering range, i.e. the distance from the sample up to which molecular layering was observed. These histograms represent the results of many approach curves.

On steel, only two layers are distinguished in the force curve, where the transition from the second to the last occurs below 0.05 nN and from the last to the substrate at about 0.1 nN.

Molecular layering was observed in 95% of the approach curves recorded on graphene and in 80% of the ones recorded on the steel substrate. A statistical evaluation of the range of tip-sample distances in which layering can be distinguished is provided in figure 2(b). The single layer graphene induces a significant increase in the layering range, its average increases from 0.8 to 2.1 nm.

We will now discuss the last layer of hexadecane on graphene, which is not displaced by the tip at forces up to 5 nN. Evidence for its stability and its structure is given by high-resolution friction force microscopy results in figure 3(a). The lateral force map reveals an arrangement of the hexadecane molecules in form of lamellae. The width of

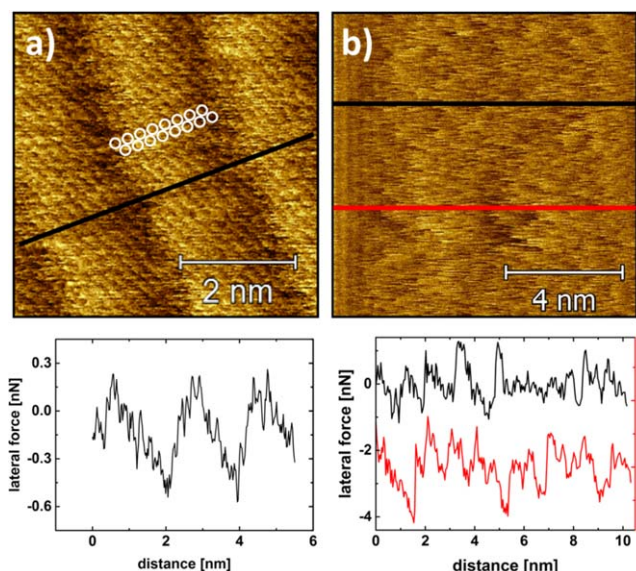


Figure 3. High-resolution lateral force maps recorded in hexadecane with a normal force of 3 nN. (a) On graphene, the adsorbed hexadecane molecules arrange in form of lamellae with a width of 2.1 nm. The cross-section was taken along the line indicated. The schematic depiction of the orientation of one hexadecane molecule is informed by the results in [21]. (b) On the steel substrate, an irregular stick-slip pattern with a characteristic slip length of about 1 nm is observed. The two cross-sections are taken the along the lines indicated in the respective color.

each lamella is 2.1 nm, close to the expected length of hexadecane. A cross-section of the lateral force indicates eight molecular-scale features across the lamella, from a structural point of view one for each ethylene group of the hexadecane molecule. The lamellae have been observed before by force microscopy [17, 20] and structural details have been resolved by scanning tunneling microscopy [21]. They have also been predicted in atomistic modeling of the adsorption [22]. In contrast, no comparable molecular order is observed in lateral force maps recorded in hexadecane on the steel substrate. We conclude that the lamellar order is induced by specific interaction of hexadecane with graphene, while the irregular stick-slip pattern in the lateral force originates in direct interaction of tip and amorphous oxidized steel surface.

4. Conclusion

A single layer of graphene on steel surfaces causes a change in the near-surface structure of the model lubricant hexadecane. Hexadecane adsorbs in an ordered layer aligned straight molecules, and this layer is stable under scanning in contact with the tip of an atomic force microscope, while no such layer is observed on the steel substrate. Graphene and hexadecane layer reduce friction at the nanoscale by a factor of three compared to the bare steel hexadecane. Furthermore, graphene introduces a pronounced structuring into four to five layers of hexadecane aligned parallel to the surface. Only two such layers are observed on the bare steel substrate. The normal load that can be borne by the last two layers in

this quasi-static boundary lubrication increases by a factor of at least 50 on graphene. These effects can be observed despite the fact the roughness of the substrate is replicated by the graphene topography. We conclude that specific interactions between the alkane chains and graphene lead to the dramatic increase in order and load-bearing capacity of the solvation forces. The enhancement of molecular layering by graphene due to specific molecular interaction has previously been reported for an ionic liquid, where the cations adsorb preferentially on graphene [23]. An enhanced layering has been observed for various liquid lubricants on graphite compared to other substrates [24], so that the effects of graphene on hexadecane can be expected to contribute also in formulated oils.

Acknowledgments

Graphene growth and transfer process was supported by an internal research program (NK218) of the Korean Institute of Machinery and Materials (KIMM). CK acknowledges support by a travel grant from the University of Science and Technology (UST).

ORCID iDs

K-S Kim  <https://orcid.org/0000-0003-4939-1973>
R Bennowitz  <https://orcid.org/0000-0002-5464-8190>

References

- [1] Kano M 2006 Super low friction of DLC applied to engine cam follower lubricated with ester-containing oil *Tribol. Int.* **39** 1682–5
- [2] Liao Y, Pourzal R, Wimmer M A, Jacobs J J, Fischer A and Marks L D 2011 Graphitic tribological layers in metal-on-metal hip replacements *Science* **334** 1687–90
- [3] Filletter T, McChesney J L, Bostwick A, Emtsev K V, Seyller Th, Horn K, Rotenberg E and Bennowitz R 2009 Friction and dissipation in epitaxial graphene films *Phys. Rev. Lett.* **102** 086102
- [4] Lee C, Li Q, Kalb W, Liu X-Z, Berger H, Carpick R and Hone J 2010 Frictional characteristics of atomically thin sheets *Science* **328** 76–80
- [5] Marsden A J, Phillips M and Wilson N R 2013 Friction force microscopy: a simple technique for identifying graphene on rough substrates and mapping the orientation of graphene grains on copper *Nanotechnology* **24** 255704
- [6] Robinson B J, Kay N D and Kolosov O V 2013 Nanoscale interfacial interactions of graphene with polar and nonpolar liquids *Langmuir* **29** 7735–42
- [7] Kim K-S, Lee H-J, Lee C, Lee S-K, Jang H, Ahn J-H, Kim J-H and Lee H-J 2011 Chemical vapor deposition-grown graphene: the thinnest solid lubricant *ACS Nano* **5** 5107–14
- [8] Berman D, Erdemir A and Sumant A V 2013 Few layer graphene to reduce wear and friction on sliding steel surfaces *Carbon* **54** 454–9
- [9] Berman D, Erdemir A and Sumant A V 2014 Graphene: a new emerging lubricant *Mater. Today* **17** 31–42
- [10] Kandanur S S, Rafiee M A, Yavari F, Schrameyer M, Yu Z Z, Blanchet T A and Koratkar N 2012 Suppression of wear in graphene polymer composites *Carbon* **50** 3178–83
- [11] Saravanan P, Selyanchyn R, Tanaka H, Fujikawa S, Lyth S M and Sugimura J 2017 Ultra-low friction between polymers and graphene oxide multilayers in nitrogen atmosphere, mediated by stable transfer film formation *Carbon* **122** 395–403
- [12] Lin J S, Wang L W and Chen G H 2011 Modification of graphene platelets and their tribological properties as a lubricant additive *Tribol. Lett.* **41** 209–15
- [13] Mungse H P and Khatri O P 2014 Chemically functionalized reduced graphene oxide as a novel material for reduction of friction and wear *J. Phys. Chem. C* **118** 14394–402
- [14] Jo K, Kim S-M, Lee S-M, Kim J-H, Lee H-J, Kim K S, Kwon Y-D and Kim K-S 2015 One-step etching, doping, and adhesion-control process for graphene electrodes *Carbon* **82** 168–75
- [15] Green C, Lioe H, Cleveland J, Proksch R, Mulvaney P and Sader J 2004 Normal and torsional spring constants of atomic force microscope cantilevers *Rev. Sci. Instrum.* **75** 1988–96
- [16] Meyer E, Hug H and Bennowitz R 2003 *Scanning Probe Microscopy: The Lab on a Tip* (Berlin: Springer)
- [17] Gosvami N N and O'Shea S J 2015 Nanoscale trapping and squeeze-out of confined alkane monolayers *Langmuir* **31** 12960–7
- [18] Gao J P, Luedtke W D and Landman U 1997 Structure and solvation forces in confined films: linear and branched alkanes *J. Chem. Phys.* **106** 4309–18
- [19] Hoth J, Hausen F, Mueser M H and Bennowitz R 2014 Force microscopy of layering and friction in an ionic liquid *J. Phys.: Condens. Matter.* **26** 284110
- [20] Pham L, Van, Kyrylyuk V, Polesel-Maris J, Thoyer F, Lubin C and Cousty J 2009 Experimental three-dimensional description of the liquid hexadecane/graphite interface *Langmuir* **25** 639–42
- [21] Zhao M, Jiang P, Deng K, Yu A-F, Hao Y-Z, Xie S-S and Sun J-L 2011 Insight into STM image contrast of n-tetradecane and n-hexadecane molecules on highly oriented pyrolytic graphite *Appl. Surf. Sci.* **257** 3247
- [22] Gobbo C, Beurroies I, Ridder D D, Eelkema R, Marrink S J, Feyter S D, van Esch J H and Vries A H D 2013 Martini model for physisorption of organic molecules on graphite *J. Phys. Chem. C* **117** 15623–31
- [23] Jurado L A and Espinosa-Marzal R M 2017 Insight into the electrical double layer of an ionic liquid on graphene *Sci. Rep.* **7** 06
- [24] Krass M-D, Krämer G, Dellwo U and Bennowitz R 2018 Molecular layering in nanometer-confined lubricants *Tribol. Lett.* **66** 87